Developmental Biology 424 (2017) 28–39

Contents lists available at ScienceDirect

Developmental Biology

journal homepage: www.elsevier.com/locate/developmentalbiology

The CapZ interacting protein Rcsd1 is required for cardiogenesis downstream of Wnt11a in *Xenopus laevis*

Annemarie Hempel[a,b], Susanne J. Kühl[a], Melanie Rothe[a,b,3], Purushothama Rao Tata[a,b,1], Ioan Ovidiu Sirbu[a,2], Seppo J. Vainio[c], Michael Kühl[a,*]

[a] Institute of Biochemistry and Molecular Biology, Ulm University, Albert-Einstein-Allee 11, D-89081 Ulm, Germany
[b] International Graduate School in Molecular Medicine Ulm, IGradU, Ulm University, 89069 Ulm, Germany
[c] Faculty of Biochemistry and Molecular Medicine, BioCenter Oulu and InfoTech Oulu,University of Oulu, Aapistie 5, FIN-90014, Finland

ARTICLE INFO

Keywords:
Cardiogenesis
Wnt11
Rcsd1

ABSTRACT

Wnt proteins are critical for embryonic cardiogenesis and cardiomyogenesis by regulating different intracellular signalling pathways. Whereas canonical Wnt/β-catenin signalling is required for mesoderm induction and proliferation of cardiac progenitor cells, β-catenin independent, non-canonical Wnt signalling regulates cardiac specification and terminal differentiation. Although the diverse cardiac malformations associated with the loss of non-canonical Wnt11 in mice such as outflow tract (OFT) defects, reduced ventricular trabeculation, myofibrillar disorganization and reduced cardiac marker gene expression are well described, the underlying molecular mechanisms are still not completely understood. Here we aimed to further characterize Wnt11 mediated signal transduction during vertebrate cardiogenesis. Using *Xenopus* as a model system, we show by loss of function and corresponding rescue experiments that the non-canonical Wnt signalling mediator Rcsd1 is required downstream of Wnt11 for ventricular trabeculation, terminal differentiation of cardiomyocytes and cardiac morphogenesis. We here place Rcsd1 downstream of Wnt11 during cardiac development thereby providing a novel mechanism for how non-canonical Wnt signalling regulates vertebrate cardiogenesis.

1. Introduction

The heart is one of the first functional organs that develops during mammalian embryogenesis. During cardiogenesis, a population of common cardiac progenitor cells is specified within the migrating anterior mesoderm that later on splits into two different cardiac lineages called the first and second heart field (FHF, SHF), respectively. While the SHF mainly contributes to the outflow tract (OFT) as well as the right ventricle and provides a minority of cells to the atria, cells of the FHF form the left ventricle and the majority of both atria (Buckingham et al., 2005). In *Xenopus,* cells of the SHF contribute to the OFT whereas cells of the FHF form the single ventricle and the two atria of the three chambered heart (Gessert and Kühl, 2009). Differentiation of cardiomyocytes of both lineages is regulated by cardiac specific transcription factors and extracellular growth factors that are interwoven into a complex gene regulatory network (Herrmann et al., 2012).

Wnt proteins can activate different, interconnected intracellular signalling branches including canonical Wnt/β-catenin and the non-canonical Wnt/JNK and Wnt/Ca^{2+} pathways (Gessert and Kühl, 2010). Through these pathways, Wnt signalling regulates diverse processes such as gene expression and cytoskeletal organisation resulting in differentiation, proliferation or cell migration. During cardiogenesis, Wnt/β-catenin signalling is required for mesoderm formation, supports proliferation of cardiac progenitor cells and inhibits terminal differentiation of cardiomyocytes. In contrast, non-canonical Wnt signalling mediated by JNK and activated by either Wnt11, Wnt5a or Wnt2 has been shown to support cardiac differentiation in several model systems including mice (Cohen et al., 2012), quails (Eisenberg and Eisenberg, 1999; Eisenberg et al., 1997), *Xenopus laevis* (Afouda et al., 2008; Pandur et al., 2002), P19 embryonic carcinoma cells (Pandur et al., 2002), murine embryonic stem cells (Chen et al., 2008; Onizuka et al., 2012; Rai et al., 2012; Terami et al., 2004; Ueno et al., 2007), human embryonic stem cells (Mazzotta et al., 2016) and different adult stem cell types (Belema Bedada et al., 2005; Koyanagi et al., 2005).

Wnt11 knockout mice are characterized by OFT defects, thinner ventricular walls, reduced ventricular trabeculation, reduced expres-

* Corresponding author.
E-mail address: michael.kuehl@uni-ulm.de (M. Kühl).
[1] Current address: Department of Cell Biology, Duke University School of Medicine, Durham, NC 27110, USA.
[2] Current address: Victor Babes University of Medicine and Pharmacy Timisoara, Biochemistry Department, 2 Eftimie Murgu, 300041 Timisoara, Romania.
[3] Tissue Homeostasis Joint-PhD-Programme between Ulm University, Germany, and University of Oulu, Finland.

http://dx.doi.org/10.1016/j.ydbio.2017.02.014
Received 21 December 2016; Received in revised form 20 February 2017; Accepted 20 February 2017
Available online 22 February 2017

sion of cardiac specific transcription factors as well as disorganized sarcomeres (Cohen et al., 2012; Nagy et al., 2010; Zhou et al., 2007). Whereas OFT defects in *Wnt11*$^{-/-}$ mice were linked to JNK/ATF2/CREBP mediated transcriptional regulation of TGFβ$_2$ (Zhou et al., 2007), the molecular mechanisms underlying the ventricular phenotypes remained elusive. In *Xenopus*, two *wnt11* genes are present with different functions during development. *Wnt11b* (formerly called Wnt11) is expressed early during cardiogenesis and is required for specification of cardiac progenitors (Afouda et al., 2008; Pandur et al., 2002). In contrast, Wnt11a (formerly called Wnt11R) is involved later during development in regulating terminal differentiation and cardiac morphogenesis (Garriock et al., 2005; Gessert et al., 2008). The effect of Wnt11a during cardiogenesis in *Xenopus* and zebrafish is at least partly mediated by the cell adhesion molecule Alcam (Choudhry and Trede, 2013; Gessert et al., 2008). Consistently, loss of either Wnt11a or Alcam leads to disturbed cardiac differentiation and morphogenesis (Choudhry and Trede, 2013; Gessert et al., 2008).

Rcsd1 (CapZ interacting protein (CapZIP) in humans or *duboraya* in zebrafish) has been shown to be an intracellular mediator of non-canonical Wnt/JNK signalling and to interact with the actin capping protein, also named CapZ (Oishi et al., 2006). CapZ binds to the barbed end of actin filaments and anchors this end of thin filaments of striated muscles at the Z-disc. In cardiomyocytes, CapZ is thereby required for proper sarcomere organisation (Frank et al., 2006). Binding of RCSD1 to CapZ is considered to prevent CapZ from binding to the actin cytoskeleton (Hernandez-Valladares et al., 2010) thereby regulating actin dynamics (Eyers et al., 2005). Binding of Rcsd1 to CapZ involves the capping protein interaction (CPI) motif of Rcsd1 (Hernandez-Valladares et al., 2010) and is regulated by phosphorylation of Rcsd1 through JNK (Eyers et al., 2005). In zebrafish, *duboraya* is expressed in cardiac tissue and its loss results in the formation of cardiac edema being indicative for cardiac malfunction (Oishi et al., 2006). Despite the occurrence of cardiac edema, the cardiac phenotype of *duboraya* deficient fish was not further analysed. Hence, we hypothesized that Rcsd1 might be involved in the non-canonical Wnt11 loss of function phenotype in the heart.

Using *Xenopus laevis* as a model system, we demonstrate that Rcsd1 and its CPI domain are required for proper cardiac development downstream of Wnt11a. Loss of either Wnt11a or Rcsd1 leads to disturbed ventricular trabeculation, reduced marker gene expression and cardiac malformations. Thus, our data places Rcsd1 downstream of Wnt11a during vertebrate cardiogenesis.

2. Methods

2.1. *Xenopus laevis* embryos

Xenopus laevis embryos were obtained and cultured according to standard protocols and staged as described by Nieuwkoop and Faber (Nieuwkoop and Faber, 1975). All procedures were performed according to the German animal use and care law and approved by the German state administration Baden-Württemberg (Regierungspräsidium Tübingen).

2.2. Protein alignment and phylogenetic tree

ClustalW2 from the EMBL-EBI homepage was used for amino acid sequence alignment, homology calculation and generation of the phylogenetic tree. Following published sequences were used: human RCSD1: NP_443094.3, mouse Rcsd1: NP_848708.2, rat Rcsd1: NP_001101819.1, chicken Rcsd1: NP_001025960.1, *X. laevis* Rcsd1: NP_001087940.1, *X. tropicalis* Rcsd1: XP_002936285.2, zebrafish Duboraya: NP_001038887.1.

2.3. Rcsd1 clones

Xenopus Rcsd1 was isolated from RNA, which was extracted from pooled embryos of different stages. The murine Rcsd1 clone was isolated from 13.5 dpc mouse embryonic heart cDNA. Deletion constructs were generated by inverse PCR using appropriate primers.

2.4. Morpholino oligonucleotide (MO) and RNA injections

All MOs were obtained by GeneTools, LLC, OR and resuspended in DEPC treated water. Wnt11a MO has been used as previously described with 30 ng per blastomere (Garriock and Krieg, 2007; Gessert et al., 2008). For Rcsd1 depletion we designed three independent MOs with the following sequences: Rcsd1_MO: 5'-CCCCTCCATTTCCTTCCTGGCTTCA-3'; Rcsd1_MO2: 5'-CCTCTCGATTCTTCGGTGCAAGTTC-3'; Rcsd1_MO3: 5'-TGATATCCGCTGATTTCCCCTCCAT-3'. For control experiments, the standard Control MO by GeneTools was used. Rcsd1 MO or Control MO were injected either unilaterally or bilaterally into one or both dorso-vegetal blastomeres at eight-cell stage to target cardiac tissue. Bilateral injections were done for analysing the heart phenotype and unilateral injections for marker gene analyses. In the later case, the uninjected side served as an internal control. 0.5 ng *gfp* RNA was co-injected in all experiments as a lineage tracer and to ensure proper injection (Dorn et al., 2014). MO concentrations for unilateral injections were: Rcsd1 MO: 10 ng; Rcsd1 MO2: 5–20 ng; Rcsd1 MO3: 5–10 ng. The functionality and efficiency of the MOs was tested by cloning of the corresponding MO binding sites in front of and in frame with GFP. For rescue experiments, 10 ng of Rcsd1 MO together with 1–2 ng RNA were injected per blastomere.

2.5. *Whole mount* in situ *hybridization (WMISH), immunohistochemistry and histological sections*

Whole mount *in situ* hybridization in *Xenopus* and mouse embryos was performed according to standard protocols (Hemmati-Brivanlou et al., 1990; Lufkin, 2007). For whole mount fluorescent immunohistochemistry the primary antibody anti Cardiac Troponin T from DSHB (University of Iowa, USA) and secondary antibody Cy3-conjugated (Dianova, Hamburg, D) were used. Embryos from WMISH experiments were embedded in gelatine blocks and sectioned with a thickness of 25 µm using a vibrating microtome, while embryos stained for cardiac Troponin T were embedded in paraffin blocks and sectioned with a thickness of 10 µm using a Leitz 1512 rotation-microtome.

2.6. RNA isolation and RT-PCR assays

Total RNA of *Xenopus* embryos was isolated from stages 1 to 25. cDNA was generated using random primers and the SuperScript II reverse transcriptase (Invitrogen, Carlsbad, CA, USA). RT-PCRs were performed using the Phire Hot Start II DNA polymerase (Thermo Scientific, Waltham, MA, USA) and following primers: gapdh_RT_forward: 5'-GCCGTGTATGTGGTGGAATCT-3'; gapdh_RT_reverse: 5'-AAGTTGTC GTTGATGACCTTTGC-3'; rcsd1_RT_forward: 5'-GACCTCTCCGTTCAG CAGTC-3'; rcsd1_RT_reverse: 5'-GCAGCTCAGATTCCTCCTTG-3'.

2.7. Cardiac explants and quantitative RT-PCR (qPCR)

Cardiac explants were dissected from embryos at stage 28 or 33/34 after bilaterally injection of either 10 ng Control or Rcsd1 MO per blastomere and 0.5 ng *gfp* as lineage tracer. Total RNA was isolated using the peq-GOLD RNApure kit (Peqlab, Erlangen, D). cDNA was generated using random primers and the SuperScript II reverse transcriptase (Life Technologies, Carlsbad, CA, USA). qPCR was performed using QuantiTec SYBR® Green PCR Kit (Qiagen, Venlo) on 20 µl LightCylcer® capillaries (Roche, Basel, Switzerland). Following primers were used: gapdh_qPCR_forward: 5'-GCCGTGTATGTGGTGGAATCT-3'; gapdh_qPCR_reverse: 5'-AAGTTGTCGTTGATGACCTTTGC-3'; myh6_qPCR_forward: 5'-CAGATCATGGGTATGCAACAACAG-3'; myh6_qPCR_reverse: 5'-ATCTGCACTGAGGTGGCTCCT-3'; tnni3_qPCR_forward: 5'-CTGCCGA CGCC ATGATG-3'; tnni3_qPCR_reverse: 5'-GTTTGAGACTGGCCC

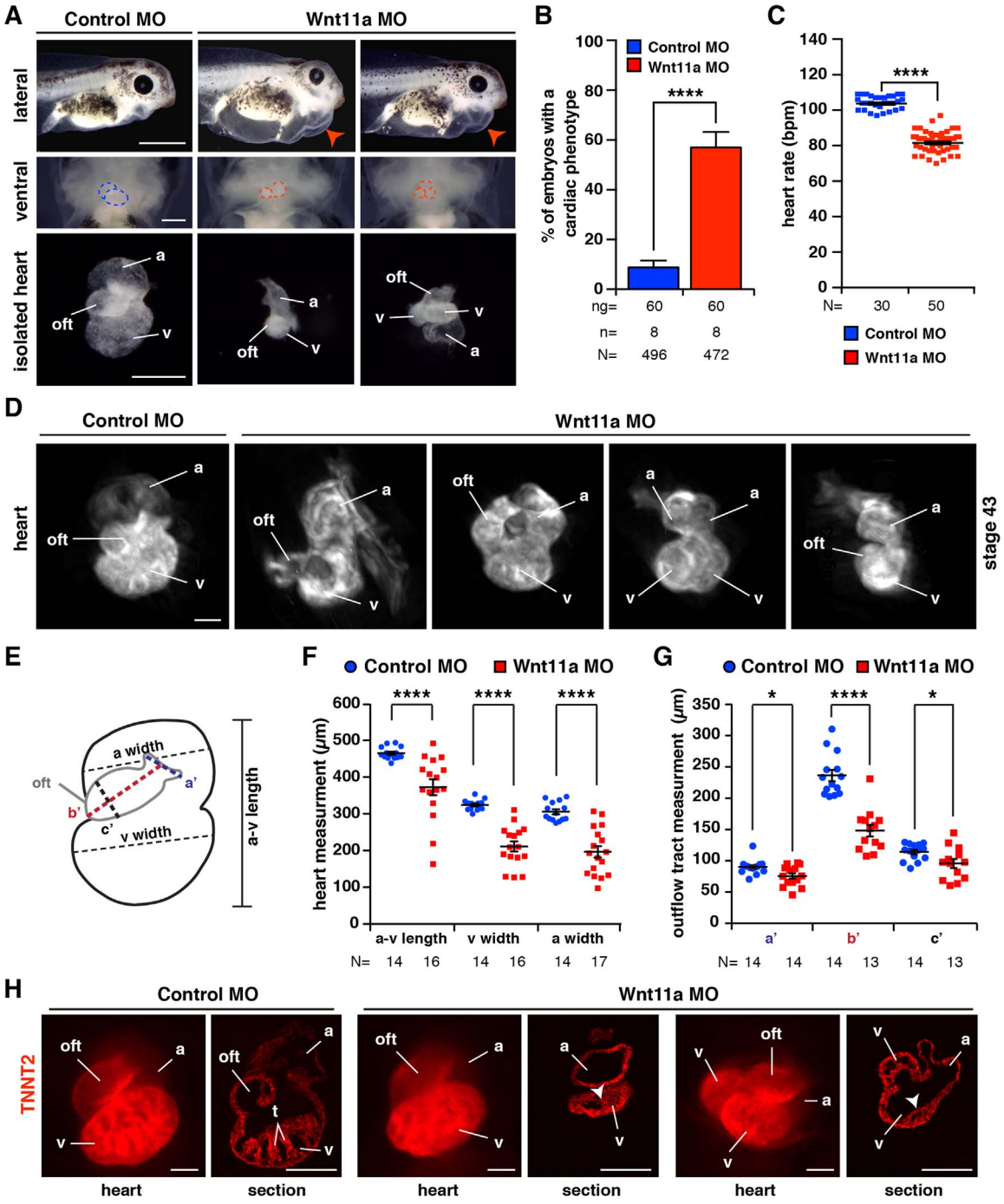

Fig. 1. : Depletion of Wnt11a disrupts cardiogenesis in *Xenopus laevis*. A. Wnt11a MO injection leads to a cardiac phenotype characterized by cardiac edema (lateral view, red arrowheads) and smaller, deformed hearts (ventral view, dotted lines; isolated hearts) at stage 43. Scale bars: lateral view: 1000 µm; ventral view and isolated hearts: 250 µm. B. Quantitative presentation of the data shown in A. C. The heart rate is significantly reduced in Wnt11a-depleted embryos. D-G. Analysis of cardiac Troponin T stained Wnt11a morphant hearts using OPT. Atrial width, ventricular width and a-v length were measured as indicated in E resulting in data provided in F. Measurement of the OFT was done as indicated in E. Data are given in G. Scale bar: 100 µm. H. Cardiac Troponin T (Tnnt2) staining shows that Wnt11a inhibition results in smaller and malformed hearts. Cross sections demonstrate a disturbed ventricular trabeculation (t). Scale bars: 100 µm. White arrowheads indicate disturbed trabeculation. a, atrium; bpm, beats per minute; n, number of independent experiments; N, number of analysed embryos; ng, nanogram; oft, outflow tract; v, ventricle. Error bars indicate standard error of the means (s.e.m.). *, p≤0.05; ****, p≤0.0001; calculated by a non-parametric Mann-Whitney rank sum test.

GTAGGT-3'. Relative gene expression was normalized against the house-keeping gene *gapdh*.

2.8. Split YFP complementation assay

Split YFP (yellow fluorescent protein) complementation assays were performed in HEK293 cells as previously described (Tecza et al., 2011). The ORFs without stop codons of murine *Rcsd1*, *Rcsd1ΔCPI*, *Rcsd1ΔNLS*, *CapZa* and *CapZb* were cloned into the pSC-B vector (Agilent Technologies, Santa Clara, CA, USA) and further in frame into pVen1 or pVen2 vectors. For negative controls the unrelated *Xenopus* Pes1 and Ppan were used (Tecza et al., 2011).

2.9. Cell culture and transfection

HEK293 and NIH3T3 cells were cultured in DMEM supplemented with penicillin (100 U/ml), streptomycin (100 mg/ml), 10% FCS at 37 °C with 5% CO_2. Cells were grown on fibronectin-coated glass cover slips. Cells were transfected with plasmids for 24 h using Lipofectamine2000 (Life Technologies, Carlsbad, CA, USA), fixed with 1x PBS, 4% PFA for 15 min and mounted in Dapi mounting medium (Dianova, Hamburg, D).

2.10. Imaging

Images of HEK293 and NIH3T3 cells were taken with a Zeiss Axiophot microscope. *Xenopus* embryos were imaged with a Leica M205FA or Olympus SZX12 microscope and sections with a Zeiss Axiophot or Olympus BX60. Images were processed using ImageJ and Adobe Photoshop CS6.

2.11. Optical projection tomography (OPT)

Optical projection tomography (OPT) was applied to obtain high-resolution three dimensional (3D) images of the heart in *Xenopus* embryos. Stage 43 embryos were fixed with Dent's fixative (DMSO and methanol, 1:4) and stained with the anti-CT3 antibody (1:50) (DSHB, Iowa USA) and Cy3-conjugated antibody 1:100 (Dianova, D). *Xenopus* embryos were mounted in 1% low melting agarose (Lonza, USA) and dehydrated overnight in 100% methanol at RT in the dark. The samples were cleared overnight at RT with benzylalcohol and benzylbenzoate (1:2) and imaged with an OPT Scanner 3001 M (Bioptonics Microscopy, UK). Pictures were taken with 1024×1024 pixel and 0.9° rotation step. The reconstruction of the data was performed using the NRecon software (SkyScan 3001). Imaris software 5.0 (Bitplane, Zurich, CH) was used to analyse OPT data.

2.12. Statistics

Quantitative presentations of data depict error bars indicating standard error of the means. P-values were calculated by a non-parametric Mann-Whitney rank sum test using GraphPad Prism 6 software.

3. Results

3.1. Loss of *Wnt11a* in Xenopus *mimics the loss of Wnt11 in mice*

We aimed to better understand the molecular mechanisms underlying the cardiac Wnt11 loss of function phenotype using *Xenopus laevis* as a model. To this end we focussed on Wnt11a that is expressed in cardiomyocytes in *Xenopus* during stages of cardiac morphogenesis and terminal differentiation comparable to the murine Wnt11 homolog (Garriock et al., 2005; Gessert and Kühl, 2009; Sinha et al., 2015). First, we asked whether loss of Wnt11a in *Xenopus* results in a phenotype similar to the Wnt11 knockout phenotype in mice and initiated a more detailed analysis of the Wnt11a morphant phenotype than previously published (Garriock et al., 2005; Gessert et al., 2008). We injected a well-described and characterized Wnt11a antisense morpholino oligonucleotide (MO) (Garriock et al., 2005; Garriock and Krieg, 2007; Gessert et al., 2008) targeting cardiac tissue, which resulted in a knockdown of endogenous Wnt11a protein. Depletion of Wnt11a led to smaller hearts with disturbed morphology including a shortened and compressed OFT (Fig. 1A,B and Suppl. Movie 1 and 2). Furthermore, Wnt11a morphant embryos revealed cardiac edema indicating an impaired cardiac function (Fig. 1A,B) and revealed a significant decrease in heart rate (Fig. 1C).

Supplementary material related to this article can be found online at http://dx.doi.org/10.1016/j.ydbio.2017.02.014.

To investigate the Wnt11a morphant heart morphology in more detail we performed 3D imaging of affected embryos using optical projection tomography (OPT) and measured the heart size. We observed a significant decrease in atrial (a) as well as ventricular (v) width as well as in a-v length (Fig. 1D-F). OPT measurements also indicated that the OFT was significantly smaller, in particular the length of the OFT was reduced (Fig. 1G). Please note, that the quantitative measurements do not represent the *in vivo* size of cardiac structures due to possible fixation/dehydration artefacts. Moreover, the variance of data also reflects the size variability of a rhythmically contracting organ (see control MO injected hearts for an example). As control MO and Wnt11a MO injected embryos were fixed and treated in parallel these data nevertheless allow for a quantification of the above described phenotypes. Cardiac Troponin T staining on sections of morphant hearts illustrated a reduced ventricular trabeculation (Fig. 1H). This was also apparent in serial sections derived from OPT images of Wnt11a MO (9 out of 14) (Suppl. Fig. 2) but not control MO (0 out of 14) (Suppl. Fig. 1) injected embryos. Garriock and colleagues (Garriock et al., 2005) described cardia bifida as one phenotype occurring in about 10% of the cases upon Wnt11a morpholino injections. Using OPT we could indeed observe duplicated heart structures in 2 out of 14 analysed embryos similar to a cardia bifida phenotype (Fig. 1D). Additionally, Wnt11a-deficient embryos revealed impaired cardiac differentiation as shown previously (Gessert et al., 2008) (Fig. 5). Taken together, this detailed description of the Wnt11a morphant phenotype indicates that loss of Wnt11a in *Xenopus* mimics several aspects of the cardiac phenotype of $Wnt11^{-/-}$ mice (Cohen et al., 2012; Nagy et al., 2010; Zhou et al., 2007). We conclude that *Xenopus* is a suitable model system to further study the effects of non-canonical Wnt signalling during terminal differentiation and morphogenesis of the heart.

3.2. Rcsd1 *is expressed in cardiac tissue*

Next, we aimed to describe the molecular mechanisms underlying the Wnt11a cardiac phenotype and searched for possible mediators of non-canonical Wnt signalling. Here we focussed on Rcsd1, since: I) Rcsd1 was shown to be expressed in cardiac progenitor cells in zebrafish, II) loss of Rcsd1 in zebrafish resulted in cardiac edema, and III) Rcsd1 had implicated to mediate non-canonical Wnt signalling (Oishi et al., 2006). A phylogenetic tree using publicly available sequences revealed a close relationship of Rcsd1 between different species (Suppl. Fig. 3A). Moreover, Rcsd1 is highly conserved across species.

For expression and functional analyses in *Xenopus*, we isolated Rcsd1 clones from different developmental stages. Interestingly, the predominant Rcsd1 variant expressed during *Xenopus* embryogenesis is C-terminally shorter than the published *Xenopus* Rcsd1 clone and the mouse homolog due to the use of an alternative splice site at the corresponding boundary between intron 6 and exon 7 (Suppl. Fig. 4). RT-PCR analysis revealed that *rcsd1* is weakly expressed maternally in *Xenopus*. Zygotic expression starts during specification of cardiac progenitor cells (stage 13) and continues till later stages (Fig. 2A). Whole mount *in situ* hybridization (WMISH) analysis indicated an expression of *rcsd1* in the common cardiac progenitor population at stage 20 (Fig. 2C,K). Expression in the cardiac mesoderm persists until later stages (Fig. 2E-N). Cross sections revealed that *rcsd1* is strongly expressed in the myocardium (Fig. 2M-N) similar to the expression of *wnt11a* in *Xenopus* (Garriock et al., 2005; Gessert and Kühl, 2009). Like in *Xenopus*, *Rcsd1* transcripts were detected in the cardiac crescent of mouse embryos at E7.7 (Fig. 2O) and at later stages in the developing murine heart (Fig. 2P,Q). These observations in *Xenopus* and mouse are similar to the cardiac expression pattern noted for the zebrafish homolog *duboraya* (Oishi et al., 2006).

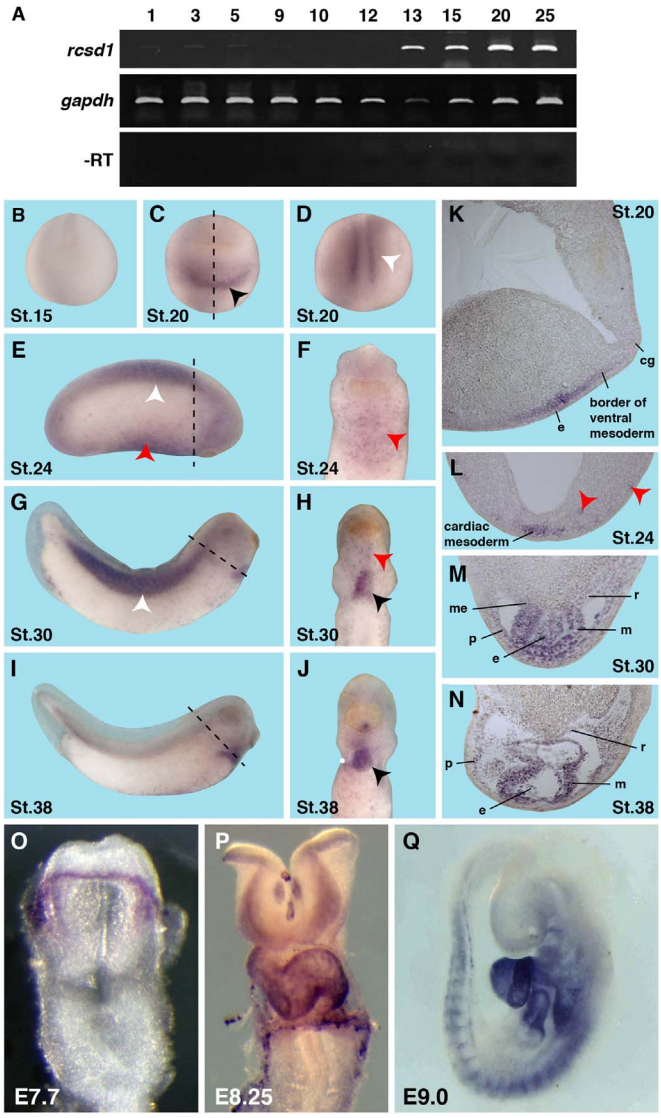

Fig. 2. : Expression of *rcsd1* during embryogenesis. A. Temporal expression of *rcsd1* at different stages of *Xenopus* development. *Gapdh* was used as loading control. Negative controls (-RT) were performed without reverse transcriptase (RT). *Rcsd1* is weakly expressed maternally. Zygotic *rcsd1* expression starts at stage 13. B-N. Spatial expression of *rcsd1* at different developmental stages as indicated in *Xenopus*. *Rcsd1* expression is first detected in the common cardiac progenitor at stage 20 (black arrowhead). Cardiac expression persists until later stages (black arrowheads). In addition, *rcsd1* transcripts were detected in the somites (white arrowheads) and myeloid cells (red arrowheads). **K-N.** Cross section through the cardiogenic region of *Xenopus* embryos as indicated by the black dashed lines in C, E, G and I, respectively. Expression in cardiac tissue is detected at stage 20 (K, sagittal section), 24 (L, transversal section), 30 (M, transversal section) and 38 (N, transversal section). e, endocardium; m, myocardium; me, mesocardium; p, pericardium; r, pericardial roof. O-Q Expression of *Rcsd1* during mouse embryogenesis. *Rcsd1* is expressed in the developing murine heart at embryonic stages E7.7 (O), E8.25 (P) and E9.0 (Q).

3.3. Loss of Rcsd1 results in cardiac defects in Xenopus

To determine whether a loss of Rcsd1 interferes with heart development, we disrupted Rcsd1 function during cardiogenesis in *Xenopus* embryos. Therefore, we relied on antisense morpholino oligonucleotides (MOs) targeting the translation start site of endogenous *rcsd1* mRNA. To exclude off-target effects, we used three different Rcsd1 MOs (one of which does not overlap with the other two) and tested their functionality prior to use (Suppl. Fig. 5). For this purpose, we cloned the corresponding MO binding sites in front of and in frame with GFP (constructs named Rcsd1 MO-GFP) and injected RNA coding for these constructs in the presence or absence of the different MOs into early *Xenopus* embryos (Suppl. Fig. 5B,C). All three Rcsd1 MOs blocked the translation of GFP indicating the functionality of these constructs. In initial loss of function (LOF) experiments, all three MOs resulted in the same phenotype as described below in more detail. For reasons of simplicity, we here show data gained with Rcsd1 MO1, further on called Rcsd1 MO throughout the manuscript. For rescue experiments, we generated a full-length *rcsd1* construct lacking the 5'UTR. As the Rcsd1 MO partially binds to the 5'UTR, the MO should not target this construct. To test this, we cloned the putative MO binding site of this construct in front of and in frame with GFP (Δ5' Rcsd1 MO-GFP). Co-injection of the MO together with RNA coding for this construct did not prevent GFP translation indicating that the above mentioned construct is not targeted by the Rcsd1 MO. This indicates that the full-length *rcsd1* construct lacking the 5'UTR can be used for rescue experiments (Suppl. Fig. 5B).

Loss of Rcsd1 function by injection of Rcsd1 MO interfered with normal cardiac development in a dose dependent manner (Fig. 3A,B). At stage 43–45, isolated hearts of Rcsd1-depleted embryos were smaller in size and showed a disturbed morphology in comparison to Control MO injected embryos (Fig. 3A, Suppl. Movie 1 and 3). We also observed cardiac edema at stages 43–45 as recently described in *duboraya* morphant fish (Oishi et al., 2006; Fig. 3A). Intriguingly, we noticed a reduced heart rate in Rcsd1 morphants (Fig. 3C) indicating that the loss of Rcsd1 results in a functional impairment of embryonic heart physiology.

Supplementary material related to this article can be found online at http://dx.doi.org/10.1016/j.ydbio.2017.02.014.

As in case of the Wnt11a morphant hearts, we also quantitatively measured the size of affected Rcsd1 morphant hearts upon OPT and found a reduced atrial width, ventricular width as well as a-v length (Fig. 3D–F). Some Rcsd1 morphant hearts initiated the looping process but failed to complete this process (9 out of 17) (Fig. 3A, right heart) or showed a duplicated or triplicated ventricle (6 out of 17) similar to a cardia bifida phenotype. Rcsd1 morphant hearts also revealed a shortened and compressed OFT (Fig. 3A, middle heart, Fig. 3G). Moreover, ventricular trabeculation was reduced and the trabeculae were located irregularly in Rcsd1-deficient embryos (Fig. 3H, white arrowhead). This was also evident in serial sections derived from OPT image stacks (Suppl. Fig. 6) (10 out of 17 embryos). Heart rate and heart morphology could be rescued by co-injecting *Xenopus* full-length *rcsd1* (Fig. 3B,C). Also trabeculation was improved upon reintroducing full-length *rcsd1* (Fig. 3H). These rescue experiments demonstrate the specificity of the Rcsd1 MO-induced cardiac phenotype. Overall these data show that Rcsd1-depleted embryos exhibit a cardiac phenotype remarkably similar to Wnt11a-deficient embryos.

3.4. Loss of Rcsd1 interferes with cardiac differentiation

Next, we were interested whether loss of Rcsd1 affects cardiac specification or differentiation and thus analysed the expression of a variety of cardiac marker genes in *Xenopus*. For this purpose, we injected the Rcsd1 MO unilaterally into embryos at 8-cell stage to target the cardiac primordium only on one side of the embryo. In this experimental setting, the un-injected side served as an internal control. As *rcsd1* is expressed in the common cardiac progenitor cell population, we first analysed the expression of *nkx2-5*, *isl1* and *tbx20* characterizing this cell population at stage 20 (Gessert and Kühl, 2009) but did not observe any significant change in marker gene expression (Fig. 4A,B). This indicates that Rcsd1 is not required for specification of cardiac progenitor cells.

Next, we investigated the expression of marker genes at stage 28 when cardiac differentiation takes place (Gessert and Kühl, 2009). Loss of Rcsd1 resulted in a down-regulation of *tbx20, tnni3, actc1, myh6* and *alcam* as shown by WMISH (Fig. 4C,D). *Tnni3, actc1, myh6* and *alcam* expression could be significantly rescued by co-injection of

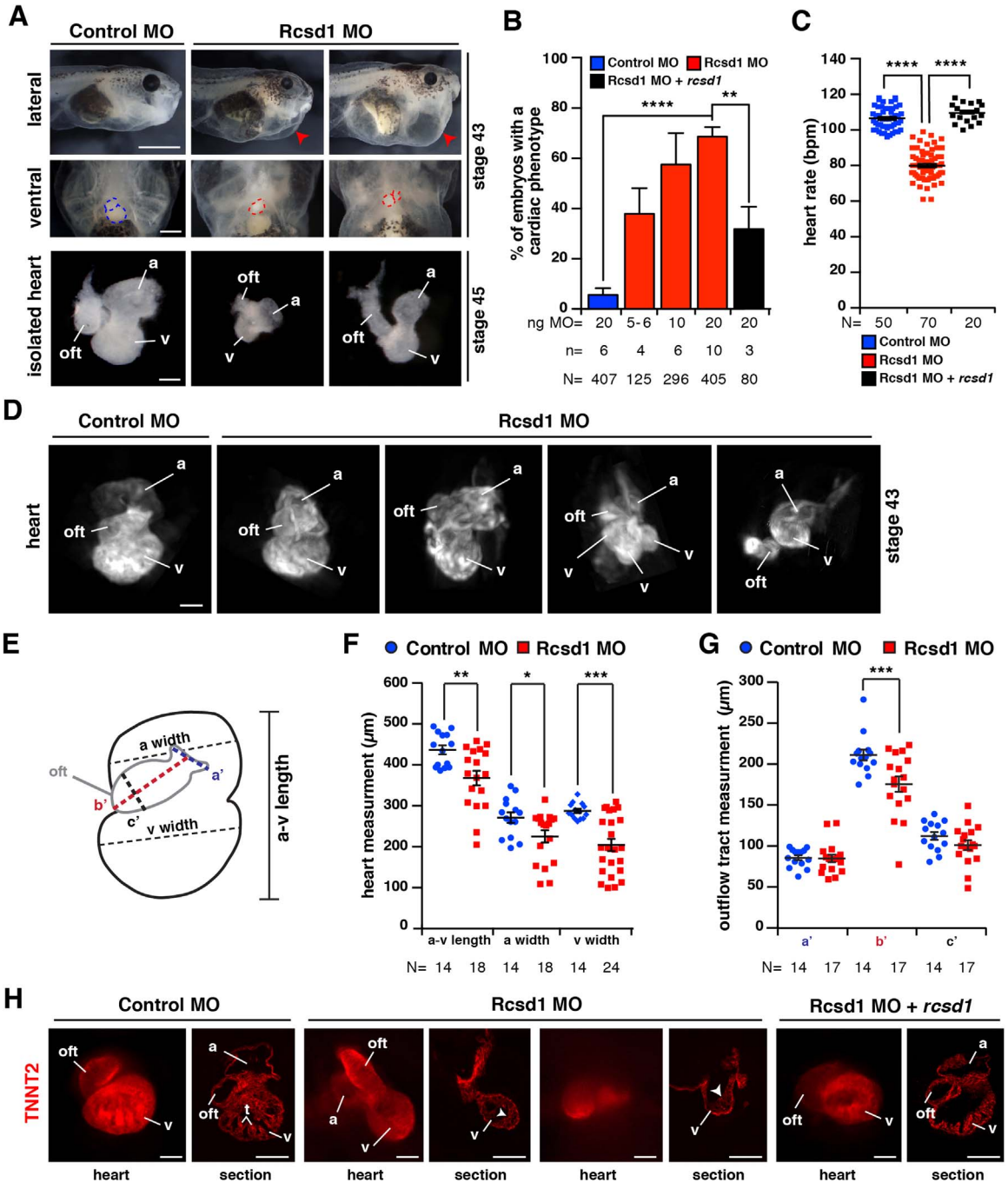

Fig. 3. : Loss of Rcsd1 phenocopies the loss of Wnt11a. A. Depletion of Rcsd1 results in a severe cardiac phenotype characterized by cardiac edema (lateral view, red arrowheads) and heart malformations (ventral view, dotted lines; isolated hearts) at indicated stages. Scale bars: lateral view: 1000 µm; ventral view: 250 µm; isolated hearts 100 µm. B. Quantitative presentation of the data shown in A at stage 43. Rcsd1 MO injection leads to a cardiac phenotype in a dose dependent manner (red columns) compared to control MO injected embryos (blue column). Co-injection of full-length *Xenopus rcsd1* RNA rescues the cardiac phenotype upon Rcsd1 deficiency (black column). C. Bilateral injection of Rcsd1 MO leads to a reduced heart rate (beats per minute, bpm) at stage 43, which is rescued by co-injecting full-length *Xenopus rcsd1* mRNA. D-G. Analysis of cardiac Troponin T stained Rcsd1 morphant hearts using OPT. Atrial width, ventricular width and a-v length were measured as indicated in E resulting in data provided in F. Measurement of the OFT was done as indicated in E. Data are given in G. Scale bar: 100 µm. H. Cardiac Troponin T (Tnnt2) staining and sectioning of Control and Rcsd1 depleted embryos at stage 43. Loss of Rcsd1 leads to malformed hearts with disturbed ventricular trabeculation (t, white arrowheads). *Rcsd1* injection restores the Rcsd1 MO induced phenotype. Scale bars: 100 µm. a, atrium; n, number of independent experiments; N, number of analysed embryos; ng, nanogram; oft, outflow tract; v, ventricle. Error bars indicate standard error of the means (s.e.m.). *, p≤0.05; **, p≤0.01; ***, p≤0.001; ****, p≤0.0001; calculated by a non-parametric Mann-Whitney rank sum test.

Xenopus full-length *rcsd1* RNA (Fig. 4G,H). Reduced expression of *tnni3* and *myh6* could be confirmed by qPCR at stages 28 and 33/34 (Fig. 4E,F). Please note that expression of *alcam*, a known target gene of Wnt11a (Choudhry and Trede, 2013; Gessert et al., 2008), was also down-regulated in Rcsd1-deficient embryos indicating that both, Wnt11a and Rcsd1, are upstream of Alcam during vertebrate heart development (Fig. 4C,D).

3.5. Rcsd1 is required downstream of Wnt11a

To probe whether Wnt11a and Rcsd1 are functionally linked during cardiogenesis, we attempted to rescue the Wnt11a phenotype by *rcsd1* RNA co-injection. Wnt11a MO injection resulted in a down-regulation of *tnni3, actc1* and *myh6* as shown earlier (Gessert et al., 2008; Fig. 5 A,B). Of note, also *rcsd1* is down-regulated upon loss of Wnt11a (Fig. 5

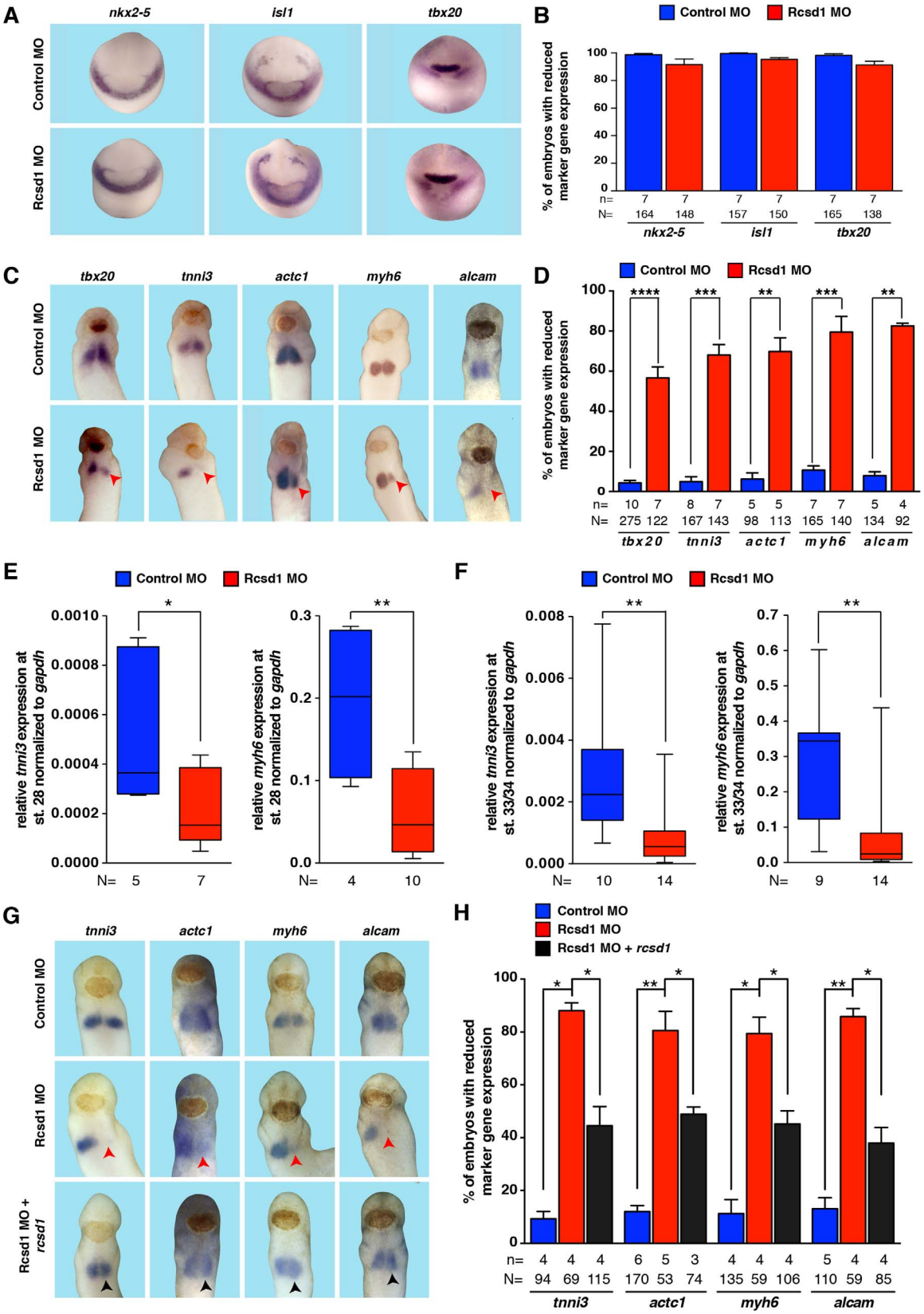

Fig. 4. : Rcsd1 depletion interferes with cardiac differentiation. A. Expression of *nkx2-5*, *isl1* and *tbx20* at stage 20 upon Rcsd1 down-regulation. B. Quantitative presentation of data shown in A. C. Unilateral injection Rcsd1 MO leads to reduced cardiac marker gene expression at stage 28 (ventral views, red arrowheads). D. Quantitative presentation of data shown in C. E-F. qPCR approaches with cardiac explants at stage 28 (E) and stage 33/34 (F) confirmed the down-regulation of *tnni3* and *myh6* upon Rcsd1 depletion. N, number of single explants used for qPCR. G. Unilateral inhibition of cardiac marker gene expression upon Rcsd1 MO injection (ventral views, red arrowheads) is restored by the co-injection of full-length *Xenopus rcsd1* RNA (ventral views, black arrowheads). H. Quantitative presentation of data shown in G. n, number of independent experiments; N, number of analysed embryos. Error bars indicate standard error of the means (s.e.m.). *, p≤0.05, **; p≤0.01; ***, p≤0.001; ****, p≤0.0001; calculated by a non-parametric Mann-Whitney rank sum test.

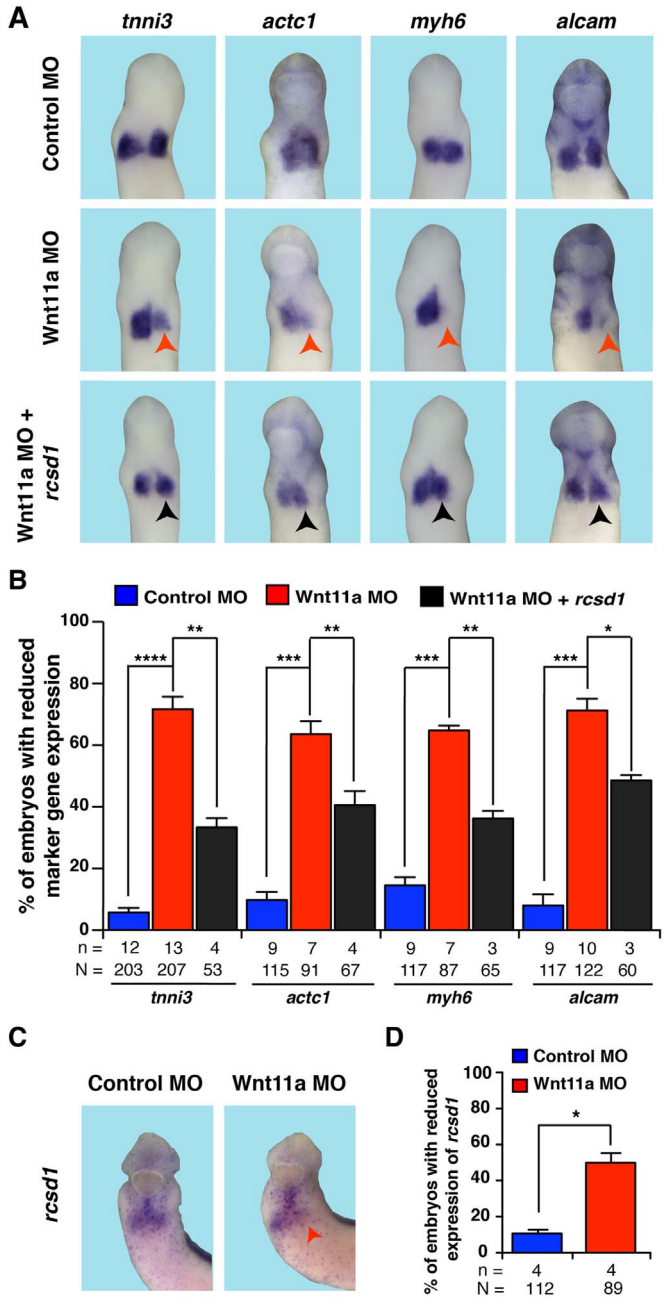

Fig. 5. : Rcsd1 acts downstream of Wnt11a. A. Unilateral injection of Wnt11a MO leads to inhibition of cardiac marker gene expression (red arrowheads), which is restored by the co-injection of *Xenopus* full-length *rcsd1* RNA (black arrowheads). B. Quantitative presentation of data shown in A. C. Unilateral injection of Wnt11a MO leads to inhibition of *rcsd1* expression (red arrowheads) D. Quantitative presentation of data shown in C. n, number of independent experiments; N, number of embryos analysed. Error bars indicate standard error of the means (s.e.m.). *, p≤0.05, **; p≤0.01; ***; p≤0.001; ****, p≤0.0001; calculated by a non-parametric Mann-Whitney rank sum test.

C,D). Co-injection of Wnt11a MO together with *Xenopus* full-length *rcsd1* mRNA reversed the loss of marker genes observed in Wnt11a morphants suggesting that Rcsd1 acts downstream of Wnt11a during cardiogenesis (Fig. 5 A,B). Interestingly, *alcam* down-regulation by loss of Wnt11a (Gessert et al., 2008) is also rescued by *rcsd1*. As *alcam* is downstream of Wnt11a (Gessert et al., 2008) and *alcam* is a direct transcriptional target of non-canonical Wnt signalling (Cizelsky et al., 2014), our data strongly suggest that Rcsd1 acts as a mediator of Wnt11a signalling in this context.

3.6. Rcsd1 interacts with CapZ in the cytoplasm via its CPI motif

To elucidate the function of Rcsd1 during vertebrate cardiogenesis in more detail, we performed cellular localization studies by overexpressing a murine EGFP-RCSD1 fusion protein in NIH3T3 cells. Expression of this fusion protein was observed in the cytosol as well as in the nucleus (Fig. 6C, upper row). One characteristic motif of Rcsd1 is the highly conserved CPI motif (Hernandez-Valladares et al., 2010; Suppl. Fig. 3B-D, Fig. 6A,B). Deletion of this motif (Rcsd1ΔCPI) resulted in exclusive localization of the protein in the cytosol (Fig. 6C, middle row). *In-silico* analysis of the Rcsd1 sequence revealed the presence of a putative nuclear localization signal (NLS) in the C-terminal part of the CPI motif (Suppl. Fig. 3B-D, Fig. 6A,B). Deletion of this short sequence in EGFP-Rcsd1 (Rcsd1ΔNLS) was sufficient to exclude Rcsd1 from the nucleus (Fig. 6C, lower row) indicating that the NLS is functional.

In order to examine whether full-length Rcsd1 and the described deletion mutants Rcsd1ΔCPI and Rcsd1ΔNLS can interact with CapZ *in vivo*, we performed a bimolecular fluorescence complementation assay (split YFP assay) (Kerppola, 2008a, 2008b; Tecza et al., 2011) using murine Rcsd1 and CapZ YFP fragment fusion constructs. CapZ is a heterodimer consisting of CapZa and CapZb subunits (Cooper and Sept, 2008). The open reading frame of Rcsd1 was fused in frame with the N-terminal part of YFP, whereas CapZa or CapZb were cloned in frame with the C-terminal part of YFP. Co-transfection of Rcsd1 and CapZa or CapZb into HEK293 cells resulted in a strong cytosolic YFP signal confirming the direct interaction between Rcsd1 with CapZa and CapZb as described earlier (Eyers et al., 2005; Hernandez-Valladares et al., 2010; Fig. 6D, E, upper rows). Deleting the CPI motif led to a loss of interaction between Rcsd1 and CapZ, whereas the deletion of the NLS had no influence on the Rcsd1-CapZ interaction (Fig. 6D, E, middle and lower rows). All fusion proteins did not interact with functionally unrelated proteins (Suppl. Fig. 7). These data show that distinct domains of Rcsd1 are required for its cellular localization and interaction with CapZ.

3.7. The CPI motif of Rcsd1 is required for Rcsd1 function during cardiogenesis

Having these data at hand provided us with the opportunity to analyse the mode of action of Rcsd1 in more detail. The injection of Rcsd1 MO led to a down-regulation of marker genes for cardiac differentiation at stage 28. This phenotype could be restored by co-injecting full-length murine *Rcsd1* (Fig. 6F,G) similar to full-length *Xenopus rcsd1* (Fig. 4G,H). In contrast, murine *Rcsd1ΔCPI* did not rescue the Rcsd1 LOF phenotype (Fig. 6F,G) suggesting that either the interaction of Rcsd1 with CapZ (Fig. 6D,E) is required for proper Rcsd1 function or that Rcsd1 functions in the nucleus during cardiogenesis since Rcsd1ΔCPI is also excluded from the nucleus (Fig. 6C). To distinguish between these two alternative hypotheses, we made use of the *Rcsd1ΔNLS* construct that is excluded from the nucleus but still interacts with CapZ (Fig. 6C–E). Co-injection of Rcsd1 MO together with *Rcsd1ΔNLS* significantly rescued the loss of Rcsd1 phenotype (Fig. 6F,G).

Finally, we investigated whether both deletion constructs were able to rescue the late cardiac phenotypes upon loss of Rcsd1 function. *Rcsd1ΔNLS* but not *Rcsd1ΔCPI* was able to rescue overall cardiac morphology (Fig. 7A,B) comparable to murine full-length *Rcsd1*. Similarly, *Rcsd1ΔNLS* but not *Rcsd1ΔCPI* partially rescued ventricular trabeculation (Fig. 7A) and heart beating rate (Fig. 7C).

In summary, these data suggest that Rcsd1 function during cardiac development depends on the interaction with CapZ but is independent of its nuclear localization.

4. Discussion

Non-canonical Wnt signalling has been earlier linked to cardiogenesis in multiple organisms during different phases such as specification

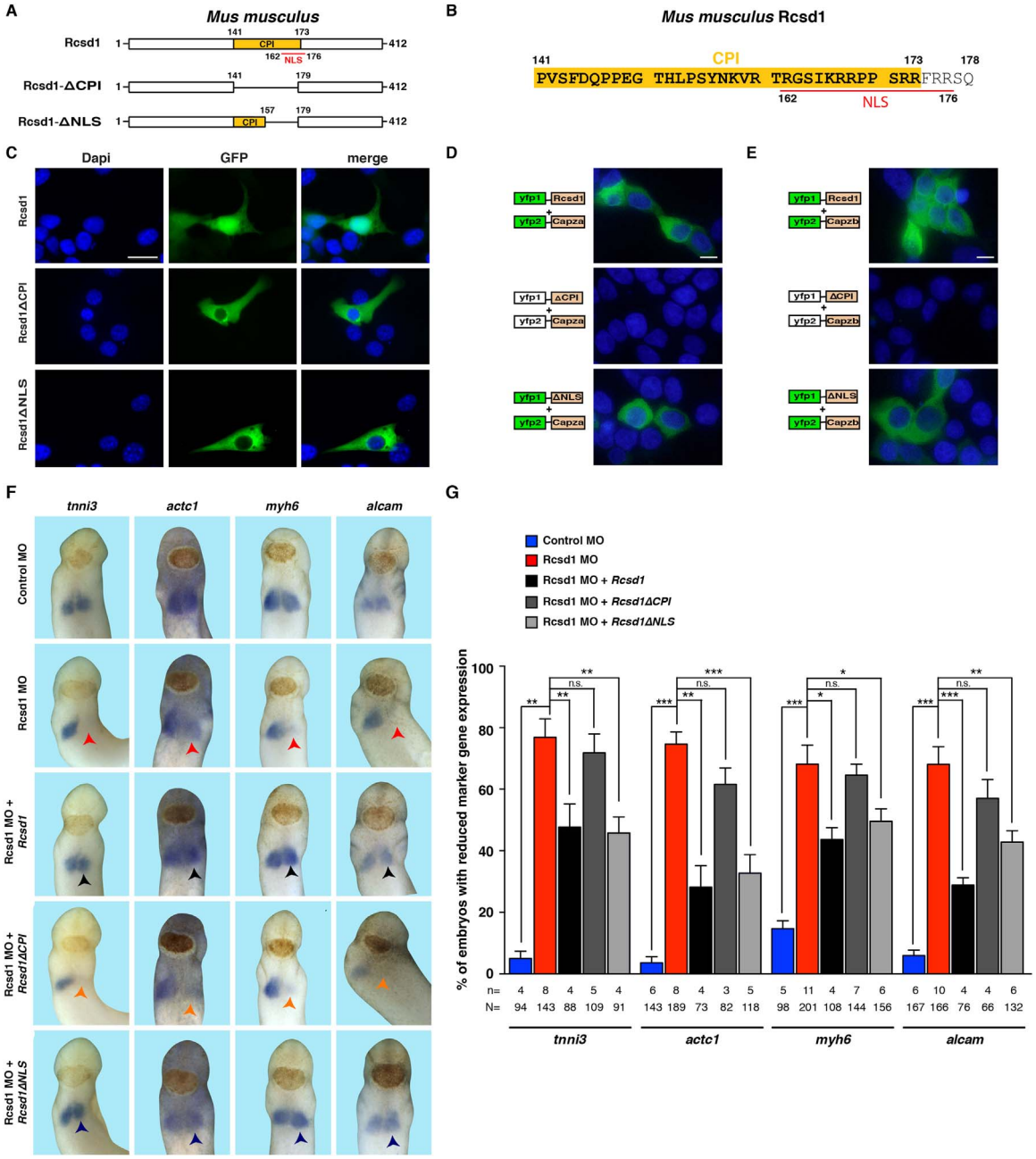

Fig. 6. : Rcsd1 functionally interacts with CapZ in the cytosol. A. Schematic overview of used murine Rcsd1 and deletion constructs. Rcsd1 contains a CPI (capping protein interaction) and a NLS (nuclear localization signal) motif. Numbers indicate amino acids in the Rcsd1 protein. B. Amino acid sequence of murine CPI and NLS motifs. Numbers indicate amino acids in the Rcsd1 protein. C. Transfection of the full-length EGFP-Rcsd1 fusion construct revealed that Rcsd1 is localized in the nucleus and cytosol (upper row). Deletion of CPI (middle row) or NLS (lower row) in Rcsd1 leads to a cytosolic localization. Scale bar: 100 µm. D-E. Split YFP complementation assays. Murine full-length Rcsd1 and Rcsd1ΔNLS (labelled as ΔNLS) interact with CapZa and CapZb whereas Rcsd1ΔCPI (labelled as ΔCPI) does not. Scale bars D, E: 10 µm. F. Rcsd1 MO was unilaterally injected along with different murine *Rcsd1* constructs and the expression of the cardiac markers *tnni3*, *actc1*, *myh6* and *alcam* was monitored at stage 28 (ventral views). Reduced marker gene expression upon loss of Rcsd1 (red arrowheads) was rescued by co-injection with the full-length murine *Rcsd1* construct (*Rcsd1*, dark grey arrowheads) and *Rcsd1ΔNLS* (dark blue arrowheads). *Rcsd1ΔCPI* however (orange arrowheads) was not able to restore marker gene expression. G. Quantitative presentation of data shown in F. n, number of independent experiments; N, number of analysed embryos. Error bars indicate standard error of the means (s.e.m.). n.s., not significant, *, p≤0.05; **, p≤0.01; ***, p≤0.001; calculated by a non-parametric Mann-Whitney rank sum test.

(Cohen et al., 2012; Onizuka et al., 2012; Pandur et al., 2002; Rai et al., 2012), terminal differentiation (Gessert et al., 2008; Nagy et al., 2010) and cardiac morphogenesis (Choudhry and Trede, 2013; Garriock and Krieg, 2007; Gessert et al., 2008; Zhou et al., 2007). Wnt11 knockout mice are characterized by smaller hearts and shortened OFTs (Cohen et al., 2012; Zhou et al., 2007), deficits in ventricular trabeculation and cardiac differentiation as well as spatially disorganized sarcomeres (Nagy et al., 2010). The molecular mechanisms involved in mediating this non-canonical Wnt signal were only rudimentary understood so far. Our study introduces Rcsd1 as a critical downstream mediator of non-canonical Wnt signalling required for these processes.

4.1. Wnt11 activates several signalling branches during cardiogenesis: potential involvement of Rcsd1

Earlier studies suggested two different signalling activities for Wnt11 function in cardiogenesis. During cardiac specification, Wnt11 (and Wnt5A) signalling can inhibit canonical Wnt/β-catenin signalling

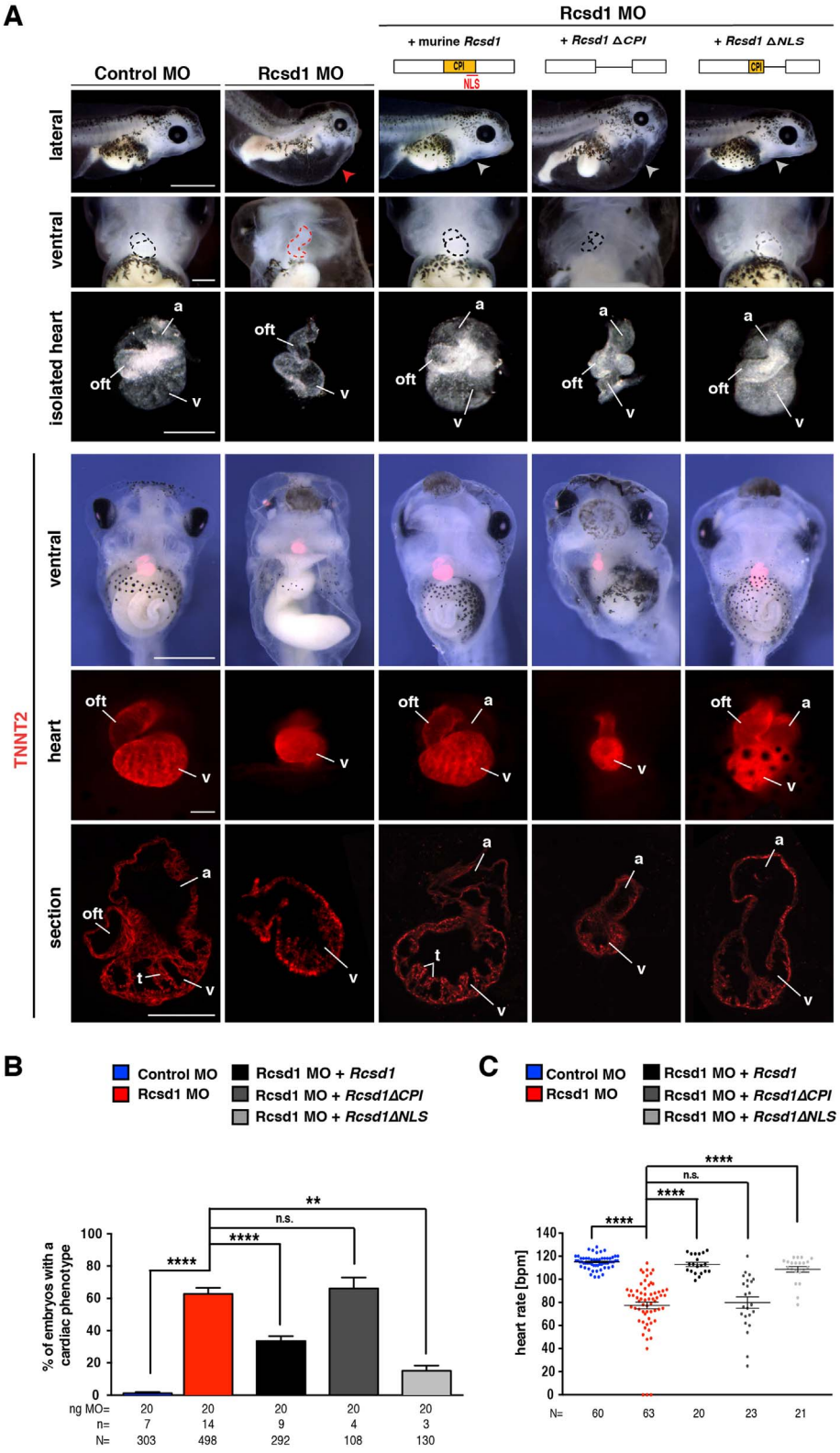

Fig. 7. : Cardiac phenotype after loss of Rcsd1 and after rescue with murine Rcsd1 constructs. A. Cardiac phenotype after Rcsd1 depletion and after rescue with murine Rcsd1 constructs at stage 43. The three upper rows show embryos from lateral and ventral view and the respective isolated hearts. The three lower rows show analysed ventricular trabeculation by cardiac Troponin T (Tnnt2) staining. Rows top to bottom: ventral view of the embryos, close-up of the respective hearts and section through the hearts cardiac phenotype after loss of Rcsd1 was rescued by co-injection with the full-length murine Rcsd1 construct and Rcsd1ΔNLS, although ventricular trabeculation was only partially restored to normal physical appearances. Rcsd1ΔCPI however was not able to restore cardiac anatomy and physiology. a, atrium; oft, outflow tract; t, trabeculae; v, ventricle, NLS: nuclear localization signal. (Lateral view: red arrowhead highlights cardiac edema upon loss of Rscd1. White arrow heads highlight the cardiac region in embryos of different rescue experiments. Scale bars: upper part: lateral view: 1000 μm; ventral view and isolated hearts: 250 μm; lower part Tnnt2: ventral view: 1000 μm; hearts and sections: 100 μm. B. Quantitative presentation of data shown in A. C. Injection of Rcsd1 MO lead to a reduced heart rate (beats per minute, bpm), which is rescued by co-injecting murine *full-length Rcsd1* or *Rcsd1ΔNLS* mRNA but not by *Rcsd1ΔCPI* mRNA. n, number of independent experiments; N, number of analysed embryos; ng, nanogram. Error bars indicate standard error of the means (s.e.m.). n.s., not significant; **, p≤0.01; ****, p≤0.0001; calculated by a non-parametric Mann-Whitney rank sum test.

(Abdul-Ghani et al., 2011; Cohen et al., 2012; Pandur et al., 2002), e.g. both factors down-regulate the Wnt/β-catenin reporter TOPFLASH during early stages of cardiac differentiation of murine ES cells (Cohen et al., 2012). The precise inhibitory mechanism of Wnt11 during specification however is not yet fully understood but activation of JNK signalling (Chen et al., 2014; Onizuka et al., 2012; Pandur et al., 2002; Rai et al., 2012) or proteases of the caspase family (Abdul-Ghani et al., 2011; Bisson et al., 2014) were discussed so far. Caspases have been shown to be able to cleave β-catenin and thus might be involved in the Wnt11 mediated inhibition of Wnt/β-catenin signalling (Abdul-Ghani et al., 2011). Our data presented here indicate that very likely, Rcsd1 is not part of this signalling cascade. First, loss of Rcsd1 in *Xenopus* does not affect cardiac specification (see Fig. 4). It is noteworthy to mention, however, that this early contribution might be obscured by the maternally expressed Rcsd1, which is not targeted by the MO approach. Second, we were not able to detect any influence of Rcsd1 on the Wnt/β-catenin signalling pathway by the use of the TOPFLASH reporter (data not shown).

Later during cardiogenesis, Wnt11 mediated JNK signalling and regulation of target genes through ATF2 transcription factors are of relevance. $TGFβ_2$ has been shown to be a target gene of this signalling branch during OFT formation in mice (Zhou et al., 2007). In *Xenopus*, zebrafish and likely human ES cells, the cell adhesion molecule Alcam is regulated through this pathway (Choudhry and Trede, 2013; Gessert et al., 2008; Mazzotta et al., 2016). Our lab showed that *alcam* is a direct target of non-canonical Wnt/JNK/ATF2 signalling (Cizelsky et al., 2014). As Rcsd1 is also a regulator of *alcam* expression and as Rcsd1 can rescue the expression of *alcam* upon loss of Wnt11a function it is likely that Rcsd1 functions as a mediator of Wnt11a function in this context.

We also observed a down-regulation of *rcsd1* on a transcriptional level upon loss of Wnt11a. Whether Rcsd1 thus is not only a mediator but also a transcriptional target of non-canonical Wnt signalling awaits further analysis. Indeed, several mediators of canonical, β-catenin mediated Wnt signalling such as Axin2, Dkk1 or Fzd7 are also direct targets of this pathway (see the Wnt homepage at http://web.stanford.edu/group/nusselab/cgi-bin/wnt/target_genes for a list of target genes and references). To our knowledge this has not yet been described for β-catenin independent signalling. It may also well be that the down-regulation of *rcsd1* in Wnt11a morphants reflects a more indirect effect as *rcsd1* has been shown to be regulated by cardiac transcription factors such as members of the GATA family (Novikov and Evans, 2013).

4.2. Insights into the molecular mechanisms of Rcsd1 function

Rcsd1 belongs to a protein family capable to interact with the capping protein (CapZ) that in turn binds to the barbed end of actin filaments thereby preventing further addition of G-actin. This interaction requires the CPI motif of Rcsd1. Our LOF studies and rescue experiments implicate Rcsd1 downstream of Wnt11a, the *Xenopus* homolog of Wnt11, during cardiogenesis. Furthermore, Rcsd1 activity requires the interaction with CapZ thereby presumably regulating the actin cytoskeleton during cardiogenesis. Proteins interacting with the capping protein have different functions, e.g. the recruitment of the active capping protein to the actin filament, the modulation of the actin cytoskeleton branching density or the inhibition of the capping protein activity thereby uncapping actin filaments (Edwards et al., 2014). Indeed, knockdown of the Rcsd1 homolog *duburaya* in zebrafish resulted in a strongly reduced F-actin network in Kupffer's vesicle (Oishi et al., 2006). As interaction of the capping protein with actin is required for modulating the apical actin network and since the actin network is required for cell movements, it is tempting to speculate whether the here observed cardiac morphological changes in Wnt11a or Rcsd1 deficient *Xenopus* hearts such as looping defects are due to changes in the actin network.

Phosphorylation of Rcsd1 by JNK reduces its affinity to CapZ. Six conserved serine residues in Rcsd1 were identified to be phosphorylated by different MAPK family members (Eyers et al., 2005). Two of these serine residues were recently linked to non-canonical Wnt/JNK signalling (Oishi et al., 2006). A full biochemical analysis of the interaction between Rcsd1 and CapZ, however, is still missing and it is not yet clear whether the phosphorylation of both serine residues is required to prevent this interaction or whether some of the other potential phosphorylations might even enhance the interaction. Sophisticated biochemical work will be required to fully understand the mode of Rcsd1 action during cardiogenesis. Finally, it remains unclear so far what the role of Rcsd1 in the nucleus might be. The presence of a highly conserved NLS implicates that the nuclear localization of Rcsd1 might be of functional relevance. Screening for interaction partners of Rcsd1 may be a starting point to further decipher the mode of Rcsd1 action in the nucleus.

5. Conclusion

We here place for the first time Rcsd1 downstream of Wnt11 during cardiac development thereby providing a novel mechanism for how non-canonical Wnt signalling regulates vertebrate cardiogenesis.

Funding

This work was supported by the Deutsche Forschungsgemeinschaft DFG (SI-1381/1-2 to IOS and Ku1166/3-2 to MK). AH, MR and PRT were supported by the International Graduate School in Molecular Medicine of Ulm University (GSC270).

Conflict of interest

None declared.

Author contributions

M.K., I.O.S. and S.V. conceived and designed the experiments. A.H., S.J.K., M.R. and P.R.T. performed the experiments. All authors analysed and discussed the data. M.K., S.J.K., A.H., M.R. drafted the manuscript. All authors commented on the manuscript.

Acknowledgement

We thank Karin Botzenhart and Petra Dietmann for their excellent technical support.

Appendix A. Supporting information

Supplementary data associated with this article can be found in the online version at doi:10.1016/j.ydbio.2017.02.014.

References

Abdul-Ghani, M., Dufort, D., Stiles, R., De Repentigny, Y., Kothary, R., Megeney, L.A., 2011. Wnt11 promotes cardiomyocyte development by caspase-mediated suppression of canonical Wnt signals. Mol. Cell. Biol. 31, 163–178.

Afouda, B.A., Martin, J., Liu, F., Ciau-Uitz, A., Patient, R., Hoppler, S., 2008. GATA transcription factors integrate Wnt signalling during heart development. Development 135, 3185–3190.

Belema Bedada, F., Technau, A., Ebelt, H., Schulze, M., Braun, T., 2005. Activation of myogenic differentiation pathways in adult bone marrow-derived stem cells. Mol. Cell Biol. 25, 9509–9519.

Bisson, J.A., Mills, B., Paul Helt, J.C., Zwaka, T.P., Cohen, E.D., 2014. Wnt5a and Wnt11 inhibit the canonical Wnt pathway and promote cardiac progenitor development via the Caspase-dependent degradation of AKT. Developmental Biology.

Buckingham, M., Meilhac, S., Zaffran, S., 2005. Building the mammalian heart from two sources of myocardial cells. nature reviews. Genetics 6, 826–835.

Chen, M., Qian, C., Bi, L.L., Zhao, F., Zhang, G.Y., Wang, Z.Q., Gan, X.D., Wang, Y.G., 2014. Enrichment of cardiac differentiation by a large starting number of embryonic

stem cells in embryoid bodies is mediated by the Wnt11-JNK pathway. Biotechnology Letters.
Chen, V.C., Stull, R., Joo, D., Cheng, X., Keller, G., 2008. Notch signaling respecifies the hemangioblast to a cardiac fate. Nat. Biotechnol. 26, 1169–1178.
Choudhry, P., Trede, N.S., 2013. DiGeorge syndrome gene tbx1 functions through wnt11r to regulate heart looping and differentiation. PLoS One 8, e58145.
Cizelsky, W., Tata, A., Kühl, M., Kühl, S.J., 2014. The Wnt/JNK signaling target gene alcam is required for embryonic kidney development. Development 141, 2064–2074.
Cohen, E.D., Miller, M.F., Wang, Z., Moon, R.T., Morrisey, E.E., 2012. Wnt5a and Wnt11 are essential for second heart field progenitor development. Development 139, 1931–1940.
Cooper, J.A., Sept, D., 2008. New insights into mechanism and regulation of actin capping protein. Int. Rev. Cell Mol. Biol. 267, 183–206.
Dorn, T., Goedel, A., Lam, J.T., Haas, J., Tian, Q., Herrmann, F., Bundschu, K., Dobreva, G., Schiemann, M., Dirschinger, R., Guo, Y., Kühl, S.J., Sinnecker, D., Lipp, P., Laugwitz, K., Kühl, M., Moretti, A., 2014. Direct Nkx2-5 transcriptional repression of Isl1 controls cardiomyocyte subtype identity. Stem cells.
Edwards, M., Zwolak, A., Schafer, D.A., Sept, D., Dominguez, R., Cooper, J.A., 2014. Capping protein regulators fine-tune actin assembly dynamics. Nat. Rev. Mol. Cell Biol. 15, 677–689.
Eisenberg, C.A., Eisenberg, L.M., 1999. WNT11 promotes cardiac tissue formation of early mesoderm. Dev. Dyn.: Off. Publ. Am. Assoc. Anat. 216, 45–58.
Eisenberg, C.A., Gourdie, R.G., Eisenberg, L.M., 1997. Wnt-11 is expressed in early avian mesoderm and required for the differentiation of the quail mesoderm cell line QCE-6. Development 124, 525–536.
Eyers, C.E., McNeill, H., Knebel, A., Morrice, N., Arthur, S.J., Cuenda, A., Cohen, P., 2005. The phosphorylation of CapZ-interacting protein (CapZIP) by stress-activated protein kinases triggers its dissociation from CapZ. Biochem. J. 389, 127–135.
Frank, D., Kuhn, C., Katus, H.A., Frey, N., 2006. The sarcomeric Z-disc: a nodal point in signalling and disease. J. Mol. Med. 84, 446–468.
Garriock, R.J., D'Agostino, S.L., Pilcher, K.C., Krieg, P.A., 2005. Wnt11-R, a protein closely related to mammalian Wnt11, is required for heart morphogenesis in Xenopus. Dev. Biol. 279, 179–192.
Garriock, R.J., Krieg, P.A., 2007. Wnt11-R signaling regulates a calcium sensitive EMT event essential for dorsal fin development of Xenopus. Dev. Biol. 304, 127–140.
Gessert, S., Kühl, M., 2009. Comparative gene expression analysis and fate mapping studies suggest an early segregation of cardiogenic lineages in Xenopus laevis. Dev. Biol. 334, 395–408.
Gessert, S., Kühl, M., 2010. The multiple phases and faces of wnt signaling during cardiac differentiation and development. Circ. Res. 107, 186–199.
Gessert, S., Maurus, D., Brade, T., Walther, P., Pandur, P., Kühl, M., 2008. DM-GRASP/ALCAM/CD166 is required for cardiac morphogenesis and maintenance of cardiac identity in first heart field derived cells. Dev. Biol. 321, 150–161.
Hemmati-Brivanlou, A., Frank, D., Bolce, M.E., Brown, B.D., Sive, H.L., Harland, R.M., 1990. Localization of specific mRNAs in Xenopus embryos by whole-mount in situ hybridization. Development 110, 325–330.
Hernandez-Valladares, M., Kim, T., Kannan, B., Tung, A., Aguda, A.H., Larsson, M., Cooper, J.A., Robinson, R.C., 2010. Structural characterization of a capping protein interaction motif defines a family of actin filament regulators. Nat. Struct. Mol. Biol. 17, 497–503.
Herrmann, F., Gross, A., Zhou, D., Kestler, H.A., Kühl, M., 2012. A boolean model of the cardiac gene regulatory network determining first and second heart field identity. PLoS One 7, e46798.
Kerppola, T.K., 2008a. Bimolecular fluorescence complementation (BiFC) analysis as a probe of protein interactions in living cells. Annu. Rev. Biophys. 37, 465–487.
Kerppola, T.K., 2008b. Bimolecular fluorescence complementation: visualization of molecular interactions in living cells. Methods Cell Biol. 85, 431–470.
Koyanagi, M., Haendeler, J., Badorff, C., Brandes, R.P., Hoffmann, J., Pandur, P., Zeiher, A.M., Kühl, M., Dimmeler, S., 2005. Non-canonical Wnt signaling enhances differentiation of human circulating progenitor cells to cardiomyogenic cells. J. Biol. Chem. 280, 16838–16842.
Lufkin, T., 2007. In situ hybridization of whole-mount mouse embryos with RNA probes: hybridization, washes, and histochemistry. CSH Protocols 2007, pdb prot4823.
Mazzotta, S., Neves, C., Bonner, R.J., Bernardo, A.S., Docherty, K., Hoppler, S., 2016. Distinctive roles of canonical and noncanonical Wnt signaling in human embryonic cardiomyocyte development. Stem Cell Rep. 7, 764–776.
Nagy, II, Railo, A., Rapila, R., Hast, T., Sormunen, R., Tavi, P., Rasanen, J., Vainio, S.J., 2010. Wnt-11 signalling controls ventricular myocardium development by patterning N-cadherin and beta-catenin expression. Cardiovasc. Res. 85, 100–109.
Nieuwkoop, P., Faber, J., 1975. External and internal stage criteria in the development of Xenopus laevis. Elsevier, Amsterdam.
Novikov, N., Evans, T., 2013. Tmem88a mediates GATA-dependent specification of cardiomyocyte progenitors by restricting WNT signaling. Development 140, 3787–3798.
Oishi, I., Kawakami, Y., Raya, A., Callol-Massot, C., Izpisua Belmonte, J.C., 2006. Regulation of primary cilia formation and left-right patterning in zebrafish by a noncanonical Wnt signaling mediator, duboraya. Nat. Genet. 38, 1316–1322.
Onizuka, T., Yuasa, S., Kusumoto, D., Shimoji, K., Egashira, T., Ohno, Y., Kageyama, T., Tanaka, T., Hattori, F., Fujita, J., Ieda, M., Kimura, K., Makino, S., Sano, M., Kudo, A., Fukuda, K., 2012. Wnt2 accelerates cardiac myocyte differentiation from ES-cell derived mesodermal cells via non-canonical pathway. J. Mol. Cell. Cardiol. 52, 650–659.
Pandur, P., Lasche, M., Eisenberg, L.M., Kühl, M., 2002. Wnt-11 activation of a non-canonical Wnt signalling pathway is required for cardiogenesis. Nature 418, 636–641.
Rai, M., Walthall, J.M., Hu, J., Hatzopoulos, A.K., 2012. Continuous antagonism by Dkk1 counter activates canonical Wnt signaling and promotes cardiomyocyte differentiation of embryonic stem cells. Stem Cells Dev. 21, 54–66.
Sinha, T., Lin, L., Li, D., Davis, J., Evans, S., Wynshaw-Boris, A., Wang, J., 2015. Mapping the dynamic expression of Wnt11 and the lineage contribution of Wnt11-expressing cells during early mouse development. Dev. Biol. 398, 177–192.
Tecza, A., Bugner, V., Kühl, M., Kühl, S.J., 2011. Pescadillo homologue 1 and Peter Pan function during Xenopus laevis pronephros development. Biol. Cell / Auspices Eur. Cell Biol. Organ. 103, 483–498.
Terami, H., Hidaka, K., Katsumata, T., Iio, A., Morisaki, T., 2004. Wnt11 facilitates embryonic stem cell differentiation to Nkx2.5-positive cardiomyocytes. Biochem. Biophys. Res. Commun. 325, 968–975.
Ueno, S., Weidinger, G., Osugi, T., Kohn, A.D., Golob, J.L., Pabon, L., Reinecke, H., Moon, R.T., Murry, C.E., 2007. Biphasic role for Wnt/beta-catenin signaling in cardiac specification in zebrafish and embryonic stem cells. Proc. Natl. Acad. Sci. USA 104, 9685–9690.
Zhou, W., Lin, L., Majumdar, A., Li, X., Zhang, X., Liu, W., Etheridge, L., Shi, Y., Martin, J., Van de Ven, W., Kaartinen, V., Wynshaw-Boris, A., McMahon, A.P., Rosenfeld, M.G., Evans, S.M., 2007. Modulation of morphogenesis by noncanonical Wnt signaling requires ATF/CREB family-mediated transcriptional activation of TGFbeta2Nat. Genet. 39, 1225–1234.